

Design for broadband high-efficiency grating couplers

Zhe Xiao,^{1,2} Feng Luan,^{1,3,*} Tsung-Yang Liow,² Jing Zhang,⁴ and Ping Shum^{1,3}

¹OPTIMUS, School of Electrical and Electronics Engineering, Nanyang Technological University, 639798, Singapore

²Institute of Microelectronics, A*STAR, 11 Science Park Road, Science Park II, 117685, Singapore

³CINTRA CNRS/NTU/THALES, UMI 3288, Research Techno Plaza, 50 Nanyang Drive, 639798, Singapore

⁴National Metrology Centre, A*STAR, 1 Science Park Drive, 118221, Singapore

*Corresponding author: luanfeng@ntu.edu.sg

Received November 1, 2011; revised December 11, 2011; accepted December 16, 2011;
posted December 20, 2011 (Doc. ID 157357); published February 8, 2012

In this Letter, we propose general optimization methods to design broadband high-efficiency grating couplers for planar waveguides. We attribute the coupling bandwidth to the mismatch of effective indices between the diffracted beam and the actual grating structure around the operation wavelength for fiber to waveguide excitation. The coupling bandwidth formula is deduced. A simple parameter-separate optimization procedure is proposed for general layered grating couplers for high coupling efficiency. Using our principle, we optimized a grating coupler for a horizontal slot waveguide operating at wavelength 1.55 μm for TM polarization. The grating coupler has 1 dB bandwidth of 60 nm and coupling efficiency of 65% with incident light from single-mode optical fiber (SMF) at 8°. © 2012 Optical Society of America

OCIS codes: 130.0130, 130.3120, 230.7390, 050.2770.

Silicon nanophotonics technologies are promising for dense photonic integration on a highly developed silicon platform by CMOS compatible technology for various on-chip processing applications [1]. Despite such positive prospects, a major obstacle lies with the coupling of light into and out of nanophotonic systems via optical fibers, since the dimensions of waveguides are much smaller than optical fibers, causing serious mode mismatch. One solution to this problem is using diffraction gratings as an out-of-plane means of coupling light into integrated photonic components. Compared to the in-plane approaches, such as inverse taper [2], grating couplers are easier to package at any position and more adapted to multiport applications.

While the coupling efficiency of grating couplers was greatly improved with many approaches, such as double-corrugation films [3], posting metal reflective mirrors or multilayer reflectors [4], and using refractive index engineered subwavelength structure [5], the coupling bandwidth mechanism is still not clear. Doerr *et al.* related the bandwidth to the fiber numerical aperture [6], which can be applied to estimate the bandwidth in the case from waveguide to fiber coupling, but there are few theoretical discussions on the intrinsic bandwidth property of grating couplers for fiber to waveguide excitation. In addition, the reported optimizations [7–10] are mostly based on a mutiparameter sweep process, and there is no general procedure to follow. In this Letter, we derive a formula to predict the achievable bandwidth for a given grating structure and propose a simplified optimization approach to maximize the coupling efficiency for general layered waveguide structures.

First we deduce a formula to calculate the grating coupling bandwidth. Equation (1) is the diffraction equation [11] of the grating coupler

$$-\frac{n_0}{\lambda} \sin \theta + \frac{n_d}{\lambda} = \frac{1}{\Lambda}, \quad (1)$$

where n_0 is the refractive index of the top cladding of the grating, n_d is defined as $|k_{d\parallel}| \lambda / 2\pi$, $k_{d\parallel}$ is the tangential

component of the wavevector of the diffracted light (diffraction order is set to be -1) along the grating surface, λ is the free-space wavelength, Λ is the grating period, and θ is incidence angle of the light. The actual effective index of a grating coupler, noted as $n_w(\lambda)$, represents the dispersion characteristic of the grating coupler. It can be calculated using the method given in previous works [12]. At the resonance wavelength λ_0 , the effective index of the diffracted light is matched to the actual grating effective index, i.e., $n_w(\lambda_0) = n_d(\lambda_0)$. For a given grating structure with fixed pitch (Λ_0) determined by the resonance wavelength λ_0 , the effective index of the diffraction light as a function of wavelength can be written as

$$n_d(\lambda) = \frac{[n_w(\lambda_0) - n_0 \sin \theta] \cdot \lambda}{\lambda_0} + n_0 \sin \theta. \quad (2)$$

$n_d(\lambda)$ has a mismatch with the actual effective index $n_w(\lambda)$, except the resonance wavelength, which is noted as $D_n(\lambda)$. Then we have

$$D_n(\lambda) = \frac{[n_w(\lambda_0) - n_0 \sin \theta] \cdot \lambda}{\lambda_0} + n_0 \sin \theta - n_w(\lambda). \quad (3)$$

Obviously, at the resonance wavelength, $D_n(\lambda_0)$ is equal to zero. Using the Taylor series expansion of Eq. (3) at the resonance wavelength and keeping the first order term of $\Delta\lambda$, we obtain

$$\Delta\lambda = \frac{\Delta D_n}{\left. \frac{n_w(\lambda_0) - n_0 \sin \theta}{\lambda_0} - \frac{dn_w(\lambda)}{d\lambda} \right|_{\lambda=\lambda_0}}. \quad (4)$$

Equation (4) relates the shift in wavelength from λ_0 to the increases of the effective index mismatch (ΔD_n), which is responsible for the coupling efficiency drop. We introduce a 1 dB mismatch coefficient $C_{1\text{dB}}$ that induces 1 dB of coupling efficiency drop; i.e.,

Table 1. The Comparison Between Different Gating Couplers

	C_I	C_{II}	C_{III}	C_{IV}
1. Λ (nm)	610	1300	630	814
2. $dn_w(\lambda)/d\lambda(\mu\text{m}^{-1})^a$	-0.457	-0.237	-0.55	-0.56
3. $\Delta\lambda_{1\text{dB}}$ by simulation	50 nm [7]	100 nm [9]	44 nm [10]	60 nm
4. $\Delta\lambda_{1\text{dB}}$ by experiment	50 nm [7]	80 nm [9]	42 nm [10]	—
5. $\Delta\lambda_{1\text{dB}}$ by Eq. (5) $C_{1\text{dB}} = 0.1$	47 nm	99 nm	46 nm	56 nm
6. η_p by simulation	66% [7]	23% [9]	36% [10]	65%

^aThe structure dispersion, which is dominant and much larger than the material dispersion, is calculated here.

$$\Delta\lambda_{1\text{dB}} = C_{1\text{dB}} \left| \frac{1}{\frac{n_w(\lambda_0) - n_o \sin \theta}{\lambda_0} - \frac{dn_w(\lambda)}{d\lambda}} \right|_{\lambda=\lambda_0}. \quad (5)$$

Equation (5) can be used to calculate the intrinsic 1 dB bandwidth of a given grating structure without detailed numerical simulations. According to Eqs. (1) and (2), the first term in the denominator in Eq. (5) is equal to $1/\Lambda_o$, which also equals the slope $dn_d(\lambda)/d\lambda$. It is clear that the denominator in Eq. (5) is the slope difference of $n_d(\lambda)$ and $n_w(\lambda)$ around resonance wavelength, which represents the mismatch between the effective indices of diffraction light and grating structure. By studying various grating couplers with different structures and materials, we find $C_{1\text{dB}}$ is about 0.10 and 0.05 for operation wavelength at $1.55 \mu\text{m}$ and $1.31 \mu\text{m}$, respectively.

Because of the fact that $n_w(\lambda_0) > n_o \sin \theta$ and $dn_w(\lambda)/d\lambda$ usually has a negative value, both terms in the denominator of Eq. (5) have to be minimized to achieve a broadband grating coupler design. The first term can be minimized by reducing the refractive index contrast between the grating coupler and the top cladding, which will result in a large grating period. The second term can be minimized by choosing a grating structure with minimal dispersion. Although the grating structure is mostly based on the waveguide to be coupled, Eq. (5) provides a useful tool to predict the potential bandwidth for a given structure without involved numerical simulations. It also suggests the possibility of introducing a transition waveguide to broaden the coupling bandwidth using a grating coupler design not constrained to the targeted waveguide. The 1 dB bandwidth given by Eq. (5) reflects the intrinsic bandwidth property of the grating coupler and does not include other factors such as the substrate, BOX layer, and top cladding. The interfaces outside the gating layers have little impact on the achievable bandwidth.

To further verify the formula, several grating couplers demonstrated in previous literature are evaluated using

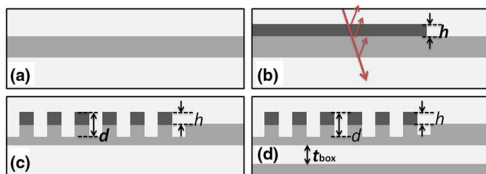


Fig. 1. (Color online) The parameter-separate optimization process. (a) Planar waveguide structure; (b) optimize the unpatterned grating region with an overlay for half film transmission; (c) scan for the best etching depth; (4) tune the external interference layers.

Eq. (5) and listed in Table 1 for comparison. C_I is a silicon grating coupler with a ploy-silicon overlay [7,8], C_{II} is a two-dimensional grating coupler with rectangle silicon teeth and a large period in the waveguide direction [9], C_{III} is a conventional grating silicon coupler [10], and C_{IV} is our proposed H-slot waveguide grating coupler, which we will present later. All the cited simulation and experiment data are provided by the literature. Through comparing row 3 to row 5, the 1 dB bandwidths calculated by Eq. (5) have a good agreement with the reported theoretical and experimental results. For the experimental result of C_{II} , the derivation comes from fabrication and experimental details [7]. The coupling efficiencies are also shown in row 6.

Equation (5) gives the design guideline for large coupling bandwidth but does not address the coupling efficiency issue. The optimization of coupling efficiency involves many parameters, which is usually a time-consuming multiparameter scanning process. Here we simplify the optimization process for grating couplers by separating optimization parameters in a sequence of steps shown in Fig. 1. We first focus on the structure with semi-infinite cladding and BOX layer, and optimize the film structure. Here we fix the duty ratio at 50% for better fabrication tolerance. Figure 1(a) is a waveguide structure to be coupled. In Fig. 1(b), first we tune the film structure so that out-of-plane percentage transmission of the unpatterned grating region is at 50%. This number is an observation from many numerical simulations for different grating structures. The optimum efficiency is always achieved with a certain film structure that gives balanced film transmission and reflection for incident waves injected at the same angle as the tilted fiber. For practical reasons, when tuning the film structure, we only add an extra overlay with tunable thickness (h) on top of the existing waveguide structure, and the refractive index of the overlay can be different from that of the waveguide layer. Taking

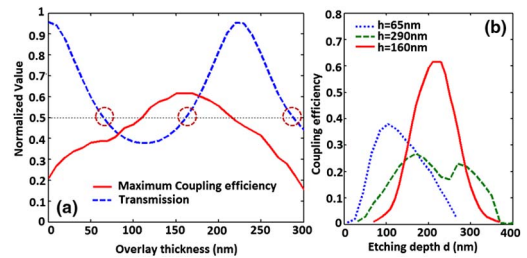


Fig. 2. (Color online) (a) The optimum coupling efficiency and film transmission at different overlay thickness. (b) The coupling efficiency versus the etching depth while overlay thickness is 65 nm, 160 nm, and 290 nm.

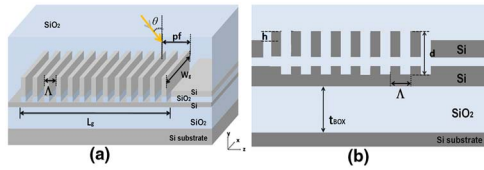


Fig. 3. (Color online) (a) Proposed grating coupler structure. (b) Schematic showing main parameters.

a recent demonstration [8] as an example, we illustrate our observations in Fig. 2(a), which shows the achievable coupling efficiency (by scanning d) and film transmission coefficient as a function of the overlay thickness h operating at $1.55 \mu\text{m}$. We can see that the maximum coupling coefficient is achieved at an h value that gives the 50% film transmission. One thing we should note is that there is more than one value of h leading to the 50% film transmission, and among them only one h value will give us the maximum coupling efficiency, which means we can use the 50% film transmission as a criteria to narrow down the optimization dimension associated with h to some (normally two or three) discrete values, which will be used in the following optimization steps.

Then, we optimize the etching depth (d) by scanning d over a reasonable region using the values of h obtained from the previous step, as shown in Fig. 1(c). This step was illustrated in Fig. 2(b), which shows the coupling efficiency versus the etching depth at three discrete values of h with 50% film transmission identified by the blue curve in Fig. 2(a). It is clear that among the three h values, the best coupling efficiency (about 60%) is achieved at $h = 160 \text{ nm}$ ($d = 220 \text{ nm}$). After the two steps mentioned above, we have achieved the optimum grating structure whose performance can be further enhanced (to a relatively small extent [8]) by adding external layers (Fig. 1(d)), such as a BOX layer or top cladding layer, or a distributed Bragg reflector (DBR). The effect of external layers is widely discussed in previous literature [4,9].

To illustrate our proposed optimization process, here we demonstrate how to optimize a grating coupler at telecom wavelengths for a horizontal slot (H-slot) waveguide [13]. The reason we choose the H-slot waveguide as the example is because the low index core layer will give us a relative low grating effective index to reduce the first term in the denominator of Eq. (5), and the layered grating structure has a comparable dispersion with a typical silicon grating coupler, so it can lead to broader coupling bandwidth. The proposed coupler structure and the main parameters are shown in Fig. 3. The coupler works at TM polarization. The refractive indices of Si and SiO_2 are 3.48 and 1.46, respectively. The waveguide section has a 50 nm SiO_2 slot layer sandwiched by two silicon slabs with a thickness of 205 nm. The fiber tilt angle is positive 8° . The film design is optimized with an overlay $h = 135 \text{ nm}$ for 50% film transmission of which the spectral is illustrated in Fig. 4(c). The etching depth d is 420 nm, which is optimized for better coupling, and the grating pitch calculated is 814 nm. Figure 4(a) indicates the coupling performance of the grating coupler. The peak efficiency of 65% with 60 nm 1 dB bandwidth is achieved for the grating coupler, while the BOX layer thickness is optimized to $3.4 \mu\text{m}$. The coupling perfor-

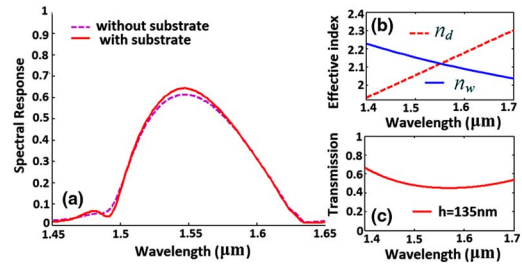


Fig. 4. (Color online) (a) The coupling efficiency of the proposed grating coupler with and without substrate. (b) The mismatch between the n_{eff} of diffraction light and the actual n_{eff} of the grating coupler. (c) Film transmission spectral of the unpatterned grating region.

mance is much better than the previously reported results [14]. Compared to the result without substrate, the coupling efficiency has only a slight 5% increase, and the bandwidth has nearly no change. Figure 4(b) shows the mismatch between the effective index n_d of the diffraction light and the real index n_w for the coupler. n_d is calculated according to Eq. (2), and n_w is calculated using the effective medium theory proposed in [12]. The slope difference is about $1.788 \mu\text{m}^{-1}$. The H-slot waveguide grating coupler has a larger coupling bandwidth while retaining a high coupling efficiency.

In summary, we have presented design approaches for broadband high-efficiency grating couplers. The coupling bandwidth formula was derived, and a simple optimization method was proposed to achieve the optimum coupling efficiency. We applied the design principles and achieved a broadband and high-efficiency H-slot waveguide grating coupler.

References

1. J. Witzens, T. Baehr-Jones, and M. Hochberg, *Nature Photonics* **4**, 10 (2010).
2. Y. Liu and J. Z. Yu, *Appl. Opt.* **46**, 7858 (2007).
3. I. A. Avrutsky, A. S. Svakhin, V. A. Sychugov, and O. Parriaux, *Opt. Lett.* **15**, 1446 (1990).
4. F. V. Laere, G. Roelkens, M. Ayre, J. Schrauwen, D. Taillaert, D. Van Thourhout, T. F. Krauss, and R. Baets, *J. Lightwave Technol.* **25**, 151 (2007).
5. R. Halir, P. Cheben, S. Janz, D.-X. Xu, Í. Molina-Fernández, and J. G. Wangüemert-Pérez, *Opt. Lett.* **34**, 1408 (2009).
6. C. R. Doerr, L. Chen, Y. Chen, and L. L. Buhl, *IEEE Photon. Technol. Lett.* **22**, 1461 (2010).
7. G. Roelken, D. Vermeulen, D. V. Thourhout, R. Baets, S. Brision, P. Lyan, P. Gautier, and J.-M. Fédéli, *Appl. Phys. Lett.* **92**, 131101 (2008).
8. G. Roelkens, D. V. Thourhout, and R. Baets, *Opt. Express* **14**, 11622 (2006).
9. X. Chen, C. Fung, Y. M. Chen, and H. K. Tsang, in *Proceedings of Conference on Lasers and Electro-Optics* (2011).
10. D. Taillaert, V. Laere, M. Ayre, W. Bogaerts, D. V. Thourhout, P. Bienstman, and R. Baets, *Jpn. J. Appl. Phys.* **45**, 6071 (2006).
11. K. G. Thomas and M. G. Moharam, *Proc. IEEE* **73**, 894 (1985).
12. S. M. Rytov, *Sov. Phys. JETP* **2**, 466 (1956).
13. V. R. Almeida, Q. Xu, C. A. Barrios, and M. Lipson, *Opt. Lett.* **29**, 1209 (2004).
14. J. V. Galan, P. Sanchis, and J. Martí, *IEEE Photon. Technol. Lett.* **20**, 985 (2008).